PHILOSOPHICAL MAGAZINE A, 2001, VOL. 81, NO. 5, 1257–1281

Parameter-free modelling of dislocation motion: the case of silicon

V. V. BULATOV†‡||, J. F. JUSTO‡§, WEI CAI‡, SIDNEY YIP‡, A. S. ARGON‡, T. LENOSKY†, M. DE KONING‡ and T. DIAZ DE LA RUBIA†

† Lawrence Livermore National Laboratory, University of California, Livermore, California 84551 USA
‡ Massachusetts Institute of Technology, Cambridge, Massachusetts, 02139, USA
§ Institute of Physics, University of São Paulo, Brazil

[*Received 10 August 2000 and accepted 5 October 2000*]

ABSTRACT

In silicon and other materials with a high Peierls potential, dislocation motion takes place by nucleation and propagation of kink pairs. The rates of these unit processes are complex unknown functions of interatomic interactions in the dislocation core, stress and temperature. This work is an attempt to develop a quantitative physical description of dislocation motion in silicon based on understanding of the core structure and the energetics of core mechanisms of mobility. Atomistic simulations reveal multiple and complex kink mechanisms of dislocation translation; however, this complexity can be rationalized through the analysis of a straight kink-free dislocation, based on symmetry-breaking arguments. Further reduction is achieved by observing that the energetics of kink mechanisms is scaled by a single parameter, the energy required to break a bond in the core. To obtain accurate values of this energy we perform density functional calculations that lead us to conclude that the low mobility of the 30° dislocation results from its high bond-breaking energy. Armed with the knowledge of kink mechanisms, we develop a kinetic Monte Carlo model that makes direct use of the atomistic data as the material-defining input and predicts the dislocation velocity on the length and time scales accessible to experiments. This provides the connection between the atomistic aspects of the dislocation core and the mobility behaviour of single dislocations.

§1. INTRODUCTION

The dislocation mobility in silicon has attracted much interest from the perspectives of electronic materials technology as well as the basic science of crystal plasticity. Since single crystals of high purity and free of defects are available, the intrinsic velocity of a single dislocation has been accurately measured over a range of temperatures and stresses. Theoretical work, on the other hand, has been based on the physical notion that dislocation motion in a crystal with high Peierls barriers takes place through the mechanism of nucleation and migration of kink pairs. Unfortunately, the ensuing model descriptions were not predictive, to the extent that quantitative interpretations of the experimental data invariably involved some

||Email: bulatov1@llnl.gov

Philosophical Magazine A ISSN 0141–8610 print/ISSN 1460-6992 online © 2001 Taylor & Francis Ltd
http://www.tandf.co.uk/journals
DOI: 10.1080/01418610110034019

degree of fitting or *ad-hoc* hypothesis. There are two challenges to the development of a fundamental framework that would allow direct modelling of the observed dislocation velocities in terms of the underlying kink kinetics. The first is that atomistic details concerning the structure and energetics of the kink defect in the dislocation core are needed. The only way to obtain this knowledge is through atomistic calculations; such results are being generated relatively recently. Secondly, a method is needed to simulate the overall dislocation movement as the cumulative effect of a large number of individual kink events. This too has been lacking.

Atomistic simulations of dislocation core structure and kinks have been attempted through the use of empirical models of interatomic interactions, such as the Keating (1966) potential which contains an undetermined term for the energy of a broken (dangling) bond, and interatomic potential models, such as Stillinger–Weber (SW) (1985) and Tersoff (1986) models, which were fitted to a wider class of physical properties. An early study by Duesbery *et al.* (1991) already revealed that the core mechanisms in silicon are quite complex. Since then the analysis of core aspects of dislocation motion in silicon has advanced to the point where all relevant kink mechanisms in the 30° and the 90° partial dislocations have been identified and catalogued (Bulatov *et al.* 1995, Nunes *et al.* 1996). Combined with the recent developments in electronic structure calculations based on the density functional theory (DFT) and the semiempirical tight-binding (TB) methods, one now has quite detailed knowledge of kink mechanisms, information which is necessary for the formulation of a parameter-free prediction of the intrinsic dislocation mobility in silicon.

The purpose of this paper is to describe a methodology, free from fitting parameters, for connecting the atomistic information on kink structure and energetics to dislocation mobility at the level of experimental observations. The discussion will be mostly based on our own studies that should be considered as work still in progress, together with a few key results obtained by other research groups. For a more comprehensive review on the topic of dislocations in Si, the reader is referred to several recent papers (Duesbery and Richardson 1991, Alexander and Teichler 1993, Lehto and Heggie 1998).

We begin with a discussion of the reconstruction of core structures of the two partial dislocations in silicon, the 30° and the 90° partials, in § 2. After briefly considering the relative role of shuffle and glide sets, one sees readily the configurational complexity associated with bond breaking, bond switching, and bond exchange as a result of energy minimization analysis, even without the presence of any kink defects. In § 3 a brief account is given of the symmetry-breaking arguments by which a complete set of the secondary core defects, kinks and reconstruction defects, can be identified *a priori*. This classification is applicable to all materials with any crystallographic structure, and the results can be useful in deciding which types of defects need to be analysed. The exploration of the atomic kink mechanisms of dislocation motion in silicon is continued in § 4. Of special interest are core defects in the 90° partial which give rise to two periodic structures. The focus in § 5 is on the particular effects of core reconstruction on dislocation mobility, established through atomistic simulations involving interatomic potentials and the density functional theory. The results discussed in §§ 2–5 constitute the atomistic information on core structure and energetics that are believed to be essential for understanding the behaviour of single dislocations on the mesoscopic level. In § 6 we describe a kinetic Monte Carlo formulation that makes direct use of the atomistic data as the material-defining input

and predicts the dislocation velocity on the length and time scales accessible to experiments. This provides the connection between the atomistic aspects of the dislocation core and the mobility behaviour of single dislocations. A brief summary and an outlook on the methodology being developed are given in § 7.

§ 2. Core structure

2.1. *Simulation methods*

Two principal components for realistic simulations of dislocations in silicon are firstly, an accurate and computationally expedient model of covalent bonding and, secondly, an efficient computational method for exploration of the multiple ways in which the atoms in the core can rebond to accommodate the displacement gradients. The very high central processing unit cost per atom per time step of the more accurate DFT calculations limits the size of the simulated system to just a few hundred atoms that can be run for just a few hundred time steps. This is inadequate for a fully dynamic simulation of dislocations. In silicon, the situation is exacerbated by high barriers for dislocation motion. Even for the most computationally 'inexpensive' (and inaccurate) empirical models of silicon due to SW and to Tersoff, using direct molecular dynamics (MD) simulations of dislocation motion have been inefficient. By necessity, most of the earlier calculations used various quasistatic techniques for finding low-energy configurations and paths for dislocation motion, for the empirical models of silicon (Heggie and Jones 1987, Duesbery *et al*. 1991, Bulatov *et al*. 1995). It was hoped that these models, however inaccurate, would reproduce some of the essential physics of dislocation motion that can be subsequently verified using more accurate approaches. In retrospect, this approach proved constructive; at present the empirical potentials are superseded by the more accurate TB models (Nunes *et al*. 1996) and, already, several principal results for dislocation mobility in silicon have been obtained using the DFT calculations (Csányi *et al*. 1998, Valladares *et al*. 1998).

For our calculations, we chose the Parrinello–Rahman (1982) version of the periodic boundary conditions for its general flexibility and robustness. Dislocations are introduced in pairs using the known elastic theory solution for the displacement field associated with a dislocation dipole. The known drawback of this direct approach is that it requires dealing with a periodic lattice of image dislocation dipoles. The lattice sum contribution to the excess energy of a dislocation dipole scales as $1/L^2$, where L is the size of the periodic supercell. For supercells containing tens of thousands of atoms this contribution can be safely ignored. On the other hand, for the relatively small supercells typically employed in the DFT calculations, the dipole lattice energy is the larger part of the excess energy and has to be evaluated very accurately. Evaluation of the image contribution to the dislocation energies is non-trivial because the lattice sums *converge only conditionally*. Several methods for dealing with such conditionally convergent sums were recently developed by Cai *et al*. (2000b). Remarkably, even for small DFT-sized supercells, it appears possible to extract the accurate core energies, provided that the supercell is large enough to avoid dislocation core overlaps.

Because of the ineffectiveness of direct MD approaches, most simulations performed so far have relied on various quasistatic methods to explore relevant details of the many-body energy landscape. Strong preference for tetrahedral bonding in silicon makes it possible to construct reasonable defect configurations based on

intuition, from the ball-and-stick models. Configurations with no or a minimum number of dangling bonds and minimal lattice distortions should have the lowest energies. Alternatively, optimal defect configurations may be found using various methods of global optimization, such as simulated annealing (Kirkpatrick 1984) or genetic algorithms (Deaven and Ho 1995). However, because dislocations themselves are metastable with respect to the perfect dislocation-free crystal, an optimization trajectory has to be confined to a region in the configuration space corresponding to a dislocated crystal. Although the mentioned search algorithms are automatic, they are statistical in nature and are not guaranteed to find the absolute optimum defect configuration. In some cases, the more intuitive approach, 'by inspection of possibilities', was found instrumental for identifying the optimal structures (Bennetto *et al.* 1997).

The brief summary of the simulation methods presented above is sketchy by design. Some of the relevant details will be given in the following sections, in connection with specific simulation results. More detailed discussions can be found elsewhere (Bulatov *et al.* 1995, Justo *et al.* 1999).

2.2. *Shuffle versus glide competition*

Dislocations in silicon have $\frac{1}{2}\langle 110\rangle$ Burgers vectors and glide in the $\{111\}$ planes. Since the diamond cubic lattice is non-primitive, two subsets of the $\{111\}$ planes can be distinguished: the widely spaced *shuffle* subset and the narrowly spaced *glide* subset. It would appear that the shuffle subset should be preferred for dislocation motion, since a unit dislocation translation requires to break only one covalent bond, as opposed to three bonds per unit translation in the glide subset. However, the glide subset has been considered more likely to contain the dislocations since it was found that dislocations in silicon are dissociated into Shockley partials. Because no stable stacking faults can exist in the shuffle subset, the glide subset appeared to be the necessary choice. Subsequent theoretical considerations supported the predominance of the glide subset, based on a γ-surface calculation by Kaxiras and Duesbery (1993) and a line tension argument by Duesbery and Joos (1996). Yet, Louchet and Thibault-Desseaux (1987) have pointed out that partials in the shuffle subset can coexist with the stacking faults in the glide subset. To move a partial from the glide position to a shuffle position, a row of atoms should be removed from or added to the extra plane terminating on the partial (figure 1). So far, high-resolution transmission electron microscopy data have neither supported nor ruled out the possibility of a mixed shuffle–glide partial core (Olsen and Spence 1981, Bourret *et al.* 1983). Direct theoretical evidence for a predominant role of the glide partials was reported by Justo *et al.* (2000) based on a combination of *ab-initio* calculations for the zero temperature energetics with classical MD simulations for the temperature-dependent free energies of the relevant core configurations. Specifically, the energetics of glide and shuffle partial dislocations were examined in a series of calculations in which the concentration of vacancies in the core of a 30° partial dislocation varied from zero for a pure glide core to 100% for a pure shuffle core. The results indicate that the equilibrium thermal concentration of vacancies in the core should be considerably higher than in the bulk crystalline environment. Still, this concentration is too low to expect that shuffle vacancy segments of appreciable length will be present in the core, supporting the view that Shockley partials in Si belong to the glide subset. This conclusion needs to be further verified for the case of the interstitial shuffle 30° partial and for the 90° partial. Even if the above conclusion stands, it

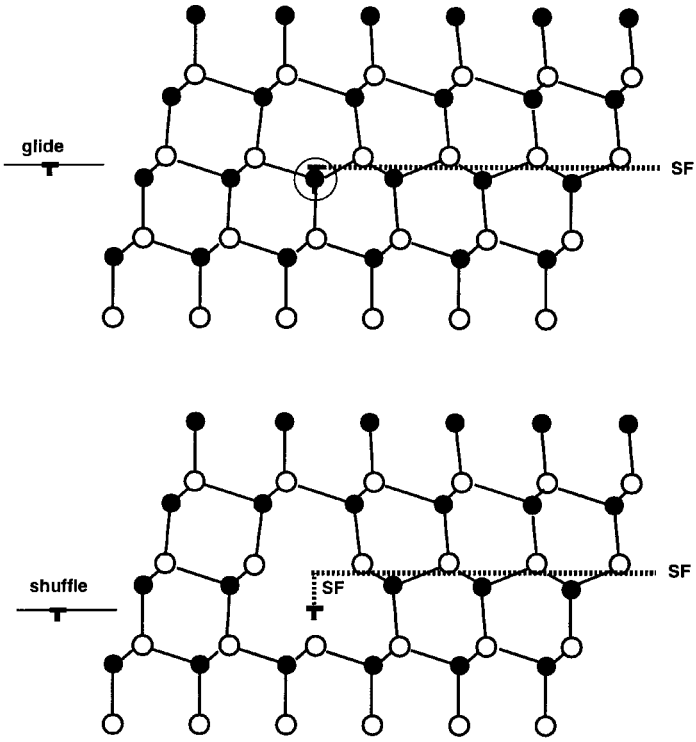

Figure 1. Shuffle and glide positions of a 30° partial dislocation in silicon. The shuffle partial is obtained by removing the row of atoms from the core.

would pertain only to the partial dislocations at rest and in local thermodynamic equilibrium. This is because vacancy or interstitial defects can be introduced into the core when dislocations move under stress, especially under conditions of point-defect supersaturation. Whether or not this principal possibility is realized in Si remains an issue for further study. In the following we shall focus exclusively on two most important dislocations in silicon: the 30° and the 90° glide partials.

2.3. *Core structure of the 30° partial dislocation*

Atomistic calculations have consistently shown that the ideal ground-state structure of the 30° partial dislocation is as shown in figure 2. In this configuration, the dangling bonds are saturated after the pairs of neighbouring core atoms move closer together to form bonded dimers. Working against this 2×1 reconstruction are relatively minor distortions of the covalent bonds; so the energy gain per reconstruction dimer is significant, ranging from 0.4 to 1.6 eV, depending on the model. Recent DFT calculations report this parameter at 0.88 eV (T. A. Arias 1997, private communication) and 1.04 eV (this work), confirming that the 2×1 reconstruction is robust. The reconstruction breaks the translational symmetry and doubles the period along the dislocation line, from b to 2b, where b is the Burgers vector magnitude of a complete $\frac{1}{2}\langle 110 \rangle$ dislocation. The reconstructed core structure is doubly degenerate; its two variants are related to each other by a half-period translation along the line. A defect must appear at the boundary between two segments reconstructed in the

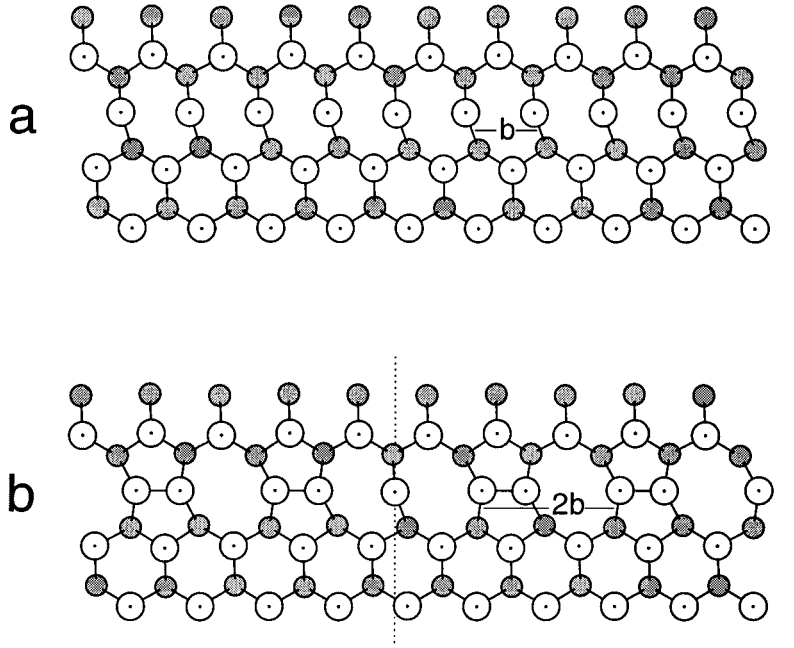

Figure 2. Core structure of a 30° partial dislocation: (*a*) unreconstructed; (*b*) reconstructed core, with a RD. Atoms above and below the glide plane are shown as open circles and full circles respectively.

opposite sense. This reconstruction defect (RD) has been also referred to as an antiphase defect by Hirsch (1979) and a soliton by Heggie and Jones (1983).

2.4. *Core structure of the 90° partial dislocation*

The driving forces for core reconstruction are the same for both partials, that is the high energy of the unsaturated dangling bonds. However, the counteracting lattice distortions are more significant in the case of the 90° partial dislocations. For the single-period (SP) core structure suggested by Hirsch (1979) (figure 3 (*a*)), the reported energy gain per reconstruction bond is generally lower than for the 30° partial dislocation, ranging from 0.3 to 1.2 eV, depending on the model. DFT calculations have not yet converged on a single acceptable value, ranging from 0.42 eV (this work) to 0.88 eV (Bigger *et al.* 1992). Emphasizing this less robust character of the 90° partial reconstruction is a recently reported alternative double-period (DP) core structure (Bennetto *et al.* 1997) (figure 3 (*b*)). The energies of the two alternative cores SP and DP, are close; the calculated differences are in the range from a few to a few tens of millielectronvolts per angstrom of dislocation line. Furthermore, which of the two structures has lower energy was shown to depend on the environment in which the dislocation is located (Lehto and Oberg 1998). Despite some differences, the results reported so far indicate that the SP and the DP cores are nearly degenerate in their energies, the implication being that they both can be involved in dislocation motion. This issue is further discussed in § 5.4.

SP core reconstruction breaks the mirror symmetry with respect to the ⟨110⟩ plane perpendicular to the line. There are two nearly degenerate types of RD which exist as a result of the symmetry breaking. Each one of them is doubly degenerate,

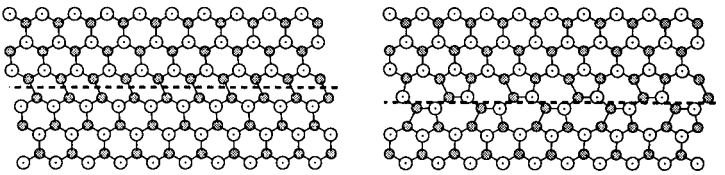

(*a*) (*b*)

Figure 3. Two alternative core reconstructions of the 90° partial: (*a*) SP reconstruction; (*b*) DP reconstruction.

having an exact mirror twin defect configuration. The situation in the DP core is more complex, because reconstruction breaks two symmetries at once: the ⟨110⟩ mirror symmetry and the translational symmetry along the line. Similar to the SP case, breaking the mirror symmetry introduces two types of RD termed *mirror solitons* by Bulatov *et al.* (1997). At the same time, similar to the 2×1 reconstruction in the 30° partial, breaking of the translation symmetry doubles the period from b to 2b and introduces a *translation soliton*. Additionally, two combinations of the translation soliton with two mirror solitons bring the total number of distinct RDs to five, four of which are doubly degenerate (Bulatov *et al.* 1997). Although RDs do not produce dislocation motion by themselves, they can interact with kinks and create large numbers of possible kink–RD combinations. The resultant mechanisms of dislocation motion in silicon can be rather complex. This complexity is further developed in the following sections.

§3. Symmetry considerations

A remarkably simple recipe was identified by Bulatov *et al.* (1997) for *a priori* classification of kinks in any given dislocation. The idea was to deduce which kink types are possible from the symmetry properties of a straight dislocation without kinks. This can be accomplished using a formal group-theoretical treatment similar to that developed by Pond (1989) for crystal interfaces. A more intuitive approach is to consider a kink pair in which, arbitrarily, one of the kinks is named the left kink (LK) and the other is named the right kink (RK) (figure 4). When a symmetry operation exists that can transform one kink into the other, the kinks are symmetry twins. This can be possible only if the host lattice and the dislocation displacement field share the symmetry in question. If the dislocation is of pure edge character, then the displacement field is symmetric with respect to a mirror plane perpendicular to the line (figure 4(*a*)). This is unless the host lattice itself lacks this mirror symmetry, in which case LK and RK must be different. If the dislocation is pure screw, then its displacement field is symmetric with respect to a 180° rotation about the dislocation axis (figure 4(*b*)). This is unless the host lattice is short of this rotation symmetry, in which case LK and RK must be different again. For a dislocation of mixed character, that is neither pure edge nor pure screw, LK and RK will be different regardless of the symmetry properties of the underlying host lattice.

Therefore, the only two cases when LK and RK should be twins are, firstly when the dislocation is pure edge and the lattice has the mirror inversion in its symmetry group or, secondly, when the dislocation is pure screw and the lattice has the 180° rotation in its symmetry group. Still, even if one of these conditions is satisfied, symmetry can break spontaneously, owing to a core reconstruction. A more detailed

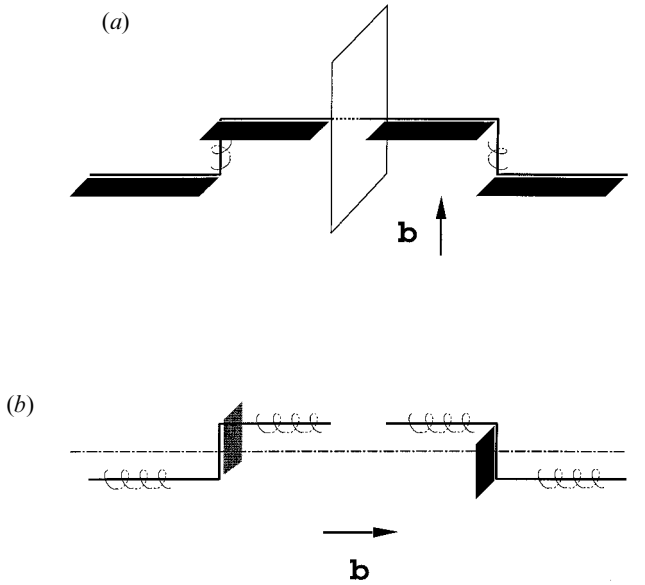

Figure 4. Displacement field of dislocation kinks viewed from above the glide plane: (*a*) mirror plane; (*b*) rotation axis. Right and left helices indicate the sense of Burgers displacement in the screw segments, while the extra half-planes inserted from above (dark) and from below (light) the glide plane show the sense of Burgers displacement in the edge segments.

discussion of various cases of symmetry breaking has been presented by Bulatov *et al.* (1997) along with a few representative examples of dislocations and kinks in different materials. Concerning dislocations in silicon, LK and RK are different in both partials, but for different reasons. In the 30° partial, LK and RK are different simply because this dislocation is of a mixed character (figure 5). The situation in the 90° partial is different. According to the symmetry test described above (figure 4 (*a*)), LK and RK should be symmetry twins in this dislocation. However, the pertinent mirror symmetry is broken by a spontaneous core reconstruction (SP or DP), making the two kinks different. In the case of SP reconstruction (figure 6) the two kinks were termed LL and RR (Nunes *et al.* 1996). As was already discussed, symmetry breaking causes RD. In the case of SP reconstruction in the 90° partial, the RDs can bind to LK and RK, bringing the total number of distinct kink species to four, each of them doubly degenerate. In the case of DP reconstruction, there are five distinct RDs that can bind to the kinks. Taking into account the degeneracy, the number of distinct kink families in the DP core becomes eight (Bennetto *et al.* 1997).

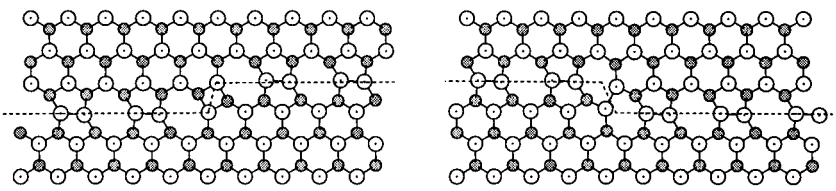

Figure 5. A pair of kinks LK and RK in a 30° partial in silicon.

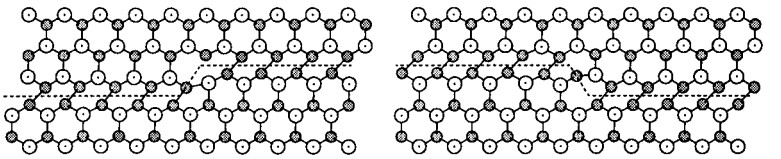

Figure 6. A pair of kinks LL and RR in a 90° partial.

The symmetry considerations are not limited to any particular material or crystallography class. Similar arguments were applied by Bulatov *et al.* (1997) to classify dislocation core defects in bcc molybdenum, in perfect agreement with the earlier atomistic study by Duesbery (1983). The usefulness of the proposed symmetry analysis is that, for any crystal lattice and for any given dislocation, the entire set of core defects and their transformations contributing to dislocation motion can be gleaned just by considering the symmetries of the host lattice and that of the straight kink-free dislocation. Since the latter can be examined with considerable accuracy using state-of-the-art first-principles calculations, the problem of identifying all relevant core defects involved in dislocation motion can be solved before actually doing any three-dimensional atomistic calculations. For our present purposes, the symmetry arguments provide an assurance that none of the important atomic modes of dislocation mobility in silicon is left unaccounted for.

§4. Atomistic kink mechanisms

The most important result of the symmetry analysis is that, for any given dislocation, we can deduce the total number and certain descriptive topological characteristics of all distinct kink and RD species. Yet, *a priori* considerations identify a core defect only as *a principal possibility* and do not say anything about its detailed structure, formation energy or stability. In fact, some of the possible species can be wholly unstable, depending on the specific model of atomic interaction (Nunes *et al* 1996, 1998). In order to examine such characteristics, three-dimensional calculations are still necessary. For these, the symmetry considerations identify precise targets.

4.1. *Core defects in the 30° partial dislocation*

Symmetry arguments can assist in setting up atomistic calculations required to evaluate core defects. As an example, consider the RDs in the 30° partial that experiences a 2×1 symmetry-breaking reconstruction. The symmetry analysis immediately shows that there is only one distinct species of such defect that is also the boundary between two segments of the same dislocation reconstructed in the opposite senses. To have exactly one RD on the periodic length of the dislocation, the latter must contain an odd number of half-periods $(2n + 1)b$, so that at least one atom with a dangling bond should be left out of the reconstruction. To ensure that the RD defect does not interact with its periodic images, n should be chosen sufficiently large, say, $n > 5$.

To 'prepare' a kink it is advantageous to use periodic supercells in which the repeat vector along the dislocation is vicinal to the direction of a Peierls valley. For example, if the repeat vector is $(a/2)[n + 1, -1, -n]$, which is vicinal to the $[1, 0, -1]$ Peierls valley, the defect-free crystal remains unaffected. However, once a dislocation dipole is introduced, each dislocation of the dipole will have one 'geometrically

necessary' kink per repeat length (figure 7). Depending on the sign of the vicinal angle and the Burgers vector, the kink will be of the LK or RK variety. When n is odd, the core will have to contain at least one dangling bond (RD) even after full 2×1 reconstruction. Provided that the geometrically necessary kink and the RD gain energy by binding to each other, a simulated annealing search should be able to find a bound kink–RD state. A sequence of configurations visited during one such search is shown in figure 8, resulting in the formation of a strongly bound LK–RD complex. The latter is one of the four distinct species of kinks anticipated from the symmetry analysis, named LC by Bulatov *et al.* (1995). The remaining fourth kink species RC is a bound state (complex) of the 'right' kink RK and the RD: RC = RK + RD. Altogether, four kink species are now identified for the 30° partial: RK, LK, RC and LC. The latter two are recognized as complexes of the two primary kinks RK and LK, with a RD.

The formation energies of the four kinks calculated using two different interatomic potentials (SW and EDIP) and an O(N) TB approach (Nunes *et al.* 1998) are contained in table 1. All three models predict that kink formation energies are rather high, ranging from 0.35 to 2.15 eV. Of the four kink species, RC and LC have higher formation energies, evidently owing to the presence of a dangling bond in their cores. Yet, these complexes should be stable against spontaneous dissociation. For example, formation energy of the RC is 0.3–0.9 eV lower than the sum of formation energies of the RK and the RD. Such relatively strong binding can be explained by partial relaxation of the bond distortions in the kink core when a dangling bond is

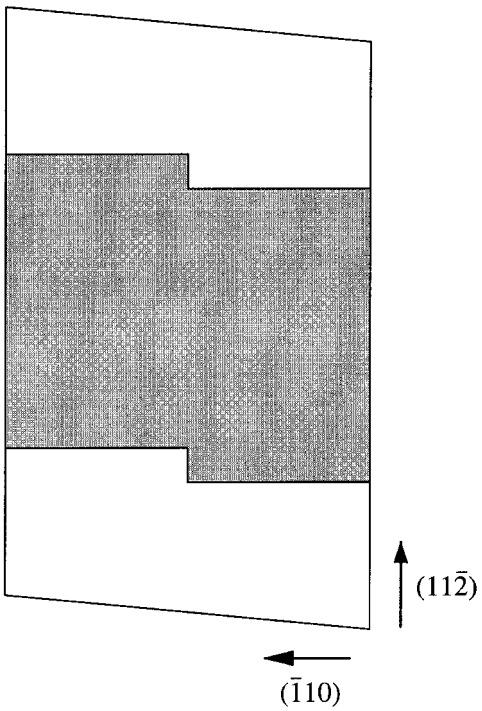

Figure 7. Projection on the {111} plane of a simulation cell in which geometrically necessary kinks are introduced in each partial of the dipole. The shaded area represents the stacking fault formed between two partial dislocations.

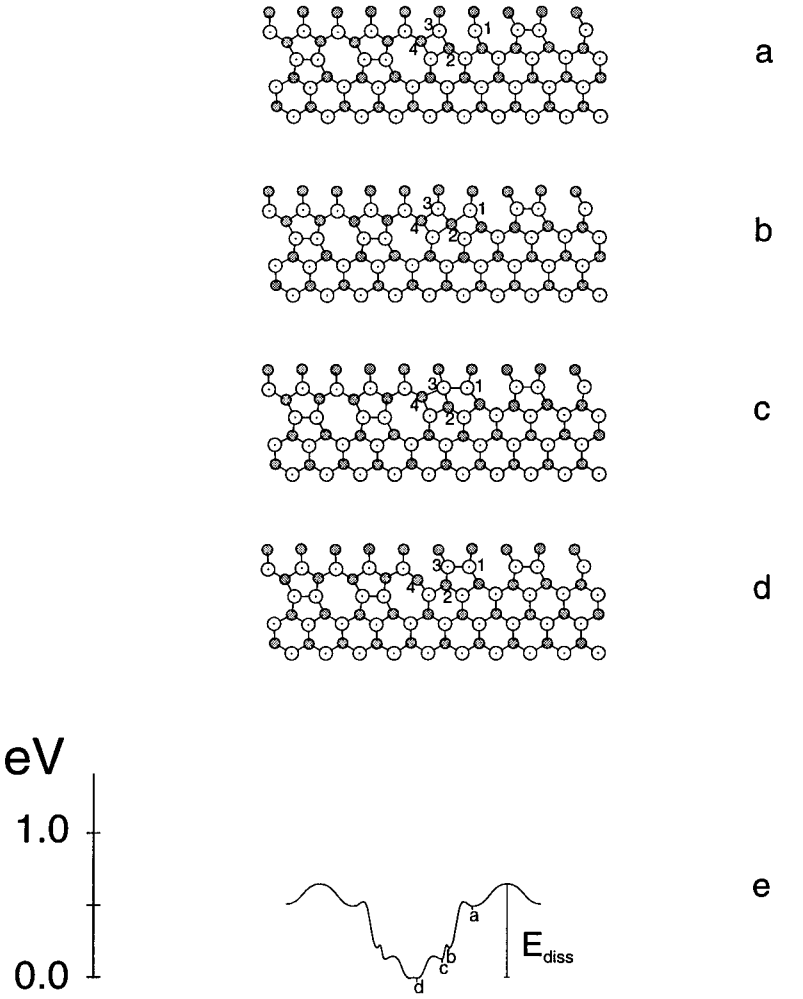

Figure 8. A simulated annealing path in which formation of a LK–RD complex was detected. The energy profile in (*e*) has markers corresponding to the energies of configurations (*a*)–(*d*) visited sequentially on the way to the final configuration (*d*).

Table 1. Kink formation energies calculated using three different models of interatomic interaction for the 30° partial.

Kink species	Formation energy (eV)		
	SW	EDIP	TB
LK	0.98	0.65	0.35
RK	0.65	0.39	1.24
LC	1.29	0.90	0.88
RC	0.63	0.83	2.15

introduced. For example, maximum bond length distortion in the fully reconstructed RK is 7%, while it is only 4% in the RC that contains a dangling bond (the data are for the SW model).

Atomistic mechanisms of kink migration in the 30° partial have been examined in detail by Bulatov *et al.* (1995). Because of the period-doubling reconstruction, kink translation paths become rather complex. For example, on its way from one low-energy configuration to another, RK visits an intermediate metastable configuration RK′, midway through the translation period (figure 9). Which of the two states, RK or RK′, has the lower energy is a subtle issue and depends on the model employed. For example, the SW model predicts that the RK energy is lower than that of RK′, whereas the EDIP model predicts the opposite. At the same time, all three models predict high migration energies for the RK kink, ranging from 0.7 to 2.1 eV. Similar to the RK case, migration of the LK kink takes place in a sequence, LK → LK′ → K → ···. Again, the predicted migration energies are high, from 0.7 to 1.5 eV. In both cases, kink migration involves a double-bond switching rearrange-

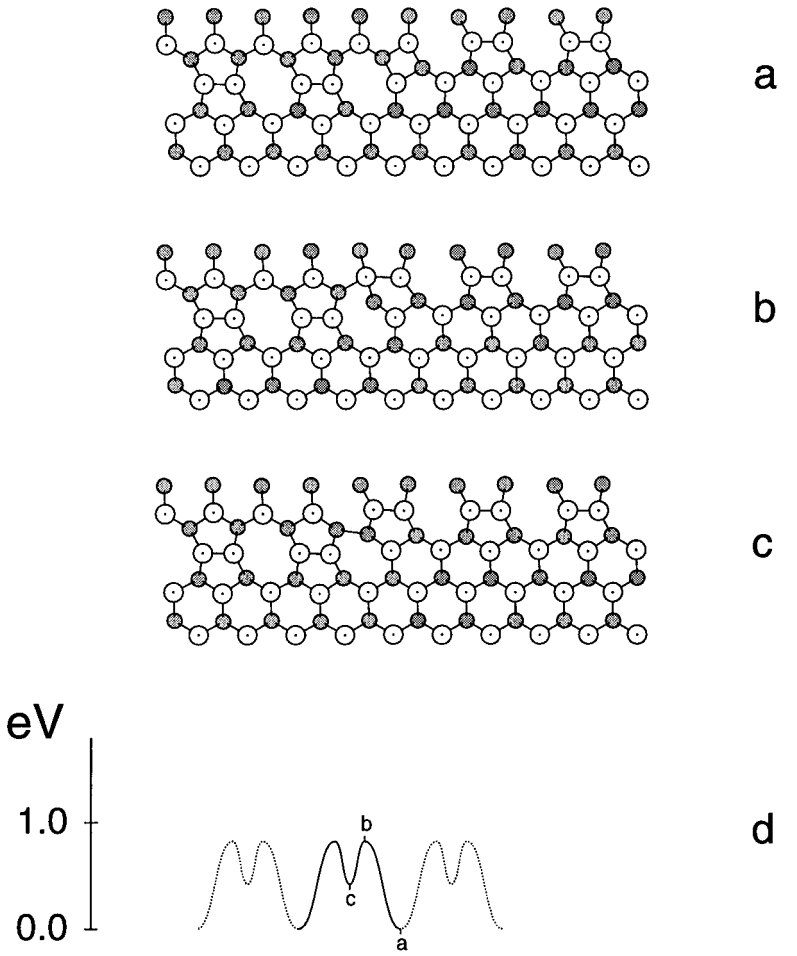

Figure 9. A low-energy path for the migration of LK.

ment in which two bonds are broken while two other bonds are formed in the process of kink translation. This is equivalent to the well known Wooten–Winer–Weaire (WWW) (1985) mechanism that preserves the tetrabonded coordination and is thought to be involved in silicon amorphization. On the contrary, translation of the two complex kinks (RC and LC) is greatly facilitated by the presence of dangling bonds involved in bond-exchange rearrangements. The resulting migration barriers are relatively low, from 0.2 to 1.0 eV.

4.2. *Core defects in the 90° partial: single period*

Breaking of the mirror symmetry in the SP core of the 90° partial introduces two different RDs and four different kinks termed LR, RL, LL and RR by Nunes *et al.* (1996). Similar to the case of 30° partial, two of the four kinks can be regarded as complexes, or bound states of two other kinks with the RDs. To some extent, which of the four kinks are regarded as primary is arbitrary. Nunes *et al.* (1996) considered LR and RL kinks as primary, since they do not contain dangling bonds and their formation energies are low. On the other hand, these two kinks are associated with a reversal in symmetry breaking, whereas the other two kinks, LL and RR, show no such reversal. Hence, these two kinks could be considered primary while the low-energy kinks LR and RL can be regarded as complexes. However, we shall follow the original classification introduced by Nunes *et al.* (1996).

Table 2 contains formation energies of all four topologically distinct kink species, calculated for the EDIP and the TB models. The formation energies of the reconstructed kinks LR and RL predicted by the TB model are notably lower than for the kinks in the 30° partial. This is probably related to the lower reconstruction energy of the 90° partial, compared to the 30° partial case. As was discussed in § 2.4, the SP reconstruction is not very robust because part of its energy gain is offset by a considerable lattice distortion required to bring the atoms to a bonding distance across the core. It appears that introduction of kinks does not add much strain to the already distorted bonds in the SP core; hence we have the low energies of kink formation. Consequently, the complex kinks LL and RR are unstable in the TB model and only marginally stable in the EDIP model, with respect to the spontaneous dissociation into one of the two low-energy (LR or RL) kinks and a RD.

Similar to the 30° partial case, translation of the reconstructed kinks LR and RL involves the double-bond switching or WWW mechanism. The resulting migration barriers range from 0.6 to 1.6 eV.

Table 2. Kink formation energies calculated using two different models of interatomic interaction for the 90° partial.

Kink species	Formation energy (eV)	
	EDIP	TB
LR	0.70	0.12
RL	0.70	0.12
LL	0.84	Unstable
RR	1.24	Unstable

4.3. *Core defects in the 90° partial: double period*

There are five different species of RDs and eight topologically distinct species of kinks in the DP core of a 90° partial. Although no systematic study of this large family of core defects has been reported, our preliminary results suggest that kink formation and migration energies are similar to those in the SP core. In particular, based on the empirical model of Tersoff (1986), we found that one of the fully reconstructed kinks in the DP core has a formation energy of 0.3 eV and a migration barrier of 2.2 eV, similar to the energies given in the preceding section for the SP core. It is relatively straightforward, using the methods described in the preceding sections, to examine the energetics of other core defects in the DP core: seven remaining kinks and five RDs. We speculate that, by analogy with the SP case, the above energies are probably representative of the other fully reconstructed kinks in the DP core. In the following section, rather than attempting to sort through the maze of all possible core defects in the DP core, we perform a simple analysis of the effect of core reconstruction on dislocation motion in silicon.

§ 5. Core reconstruction and dislocation mobility

5.1. *Reconstruction bonds and the energetics of kink mechanisms*

Dislocation translation requires breaking and making of covalent bonds. Ultimately, it is the energetics of bond breaking that should define lattice resistance to dislocation motion. Of the bonds involved in dislocation translation, reconstruction bonds are most distorted and, consequently, least strong. A direct way to quantify the contribution of reconstruction bonds to the lattice resistance would be to examine the energetics of kink mechanisms for a range of systems with different strengths of the reconstruction bonds. Such an investigation, however difficult, could have clarified the observed variations of intrinsic dislocation mobility over the family of elemental and compound semiconductor materials (Kirchner and Suzuki 1998).

A much simpler approach was taken by Justo *et al.* (1999). The idea was, using the same empirical model, to suppress core reconstruction artificially and to compare kink mechanisms in the 'so-designed' unreconstructed core with the reconstructed kink mechanisms discussed in the preceding sections. Utilizing one's ability to control numerical simulation, such a comparison has no realistic analogue and yet it allows better appreciation of the contribution of core reconstruction to the lattice resistance.

Various unreconstructed core configurations were reported in our earlier calculations based on the empirical potentials of the SW (Bulatov *et al.* 1995) and the EDIP (Justo *et al.* 1998) methods. Those typically corresponded to high-energy local minima separated by small barriers from low-energy 'reconstructed' states. Sometimes it was even possible to introduce kinks and move them along the line, still keeping the core atoms from reconstruction. This, possibly unphysical tendency of the empirical models was explored by Justo *et al.* (1999) where a series of calculations was performed of kink migration and formation energies in the unreconstructed cores of 90° and 30° partial dislocations. The results obtained for the SW and the EDIP models suggest that the contribution of reconstructed bonds to kink energetics in silicon is large, especially for kink migration barriers. For example, for the SW model the barrier for the kink migration mechanism depicted in figure 9 is 0.74 eV. However, the barrier for the same mechanism in the unconstructed core is only 0.3 eV. The corresponding values of 1.2 and 0.3 eV were obtained for the EDIP

model, confirming that reconstruction bond contribution to migration barriers is large.

While the accuracies of the two empirical models can be questioned, their agreement indicates that, at least in silicon, core reconstruction should have bearing on the energetics of kink mechanisms. This echoes an old argument that the energy of the dimer bond in the core is an important parameter. Based on the results discussed by Justo *et al.* (1999), it appears that this same energy is a relevant scaling parameter for the lattice resistance to dislocation motion.

5.2. *Reconstruction energetics from first principles*

The energy required to break a reconstruction bond is the same as the energy reduction per bond caused by core reconstruction. The latter can be calculated using relatively small periodic supercells with the depth of only one or two lattice spacings along the line. This permits more accurate calculations using the TB (Bennetto *et al.* 1997) and the DFT (Valladares *et al.* 1998) methods. One of the first such calculations was reported in a paper by the Oxford–Cambridge group (Bigger *et al.* 1992). The results showed that the symmetry-breaking core reconstruction in the 90° partial (SP) is robust, leaving no deep electronic states inside the bandgap. The reported reconstruction energy per dimer bond was 0.87 eV. More recently a similar value of 0.88 eV per bond was obtained for the 30° partial (T. A. Arias 1997, private communication). It should be noted that, in obtaining these values for the reconstruction energies, the two groups (Bigger *et al.* 1992, T. A. Arias 1997, private communication) used different pseudopotentials, supercells and other computational parameters. We decided to revisit the issue of the relative strength of core reconstruction in two partials, using identical computational settings for both partial dislocations. For that we employed the Vienna *Ab-initio* Simulation Package (VASP) plane-wave pseudopotential code developed at the Technical University of Vienna (Kresse and Hafner 1993). This code implements the Vanderbilt (1990) ultrasoft pseudopotential scheme, as supplied by Kresse and Hafner (1994). Initially, in an attempt to calibrate our calculations against the earlier results, we repeated the calculations using exactly the same supercells as were originally employed by Bigger *et al.* (1992) for the 90° partial and by T. A. Arias (1997, private communication), for the 30° partial. The resulting reconstruction energy for the 30° partial was 1.02 eV per bond, somewhat higher than 0.88 eV per bond reported by T. A. Arais (1997, private communication). However, for the 90° partial we obtained a value of 0.42 eV per bond, significantly lower than 0.87 eV per bond reported by Bigger *et al.* (1992).

In order to check what could have caused such a discrepancy we examined numerical convergence with respect to the supercell size, energy cut-off value and the number of k points. For the case of SP reconstruction in the 90° partial, periodic supercells ranging in size from 64 to 216 atoms were employed. Additionally, the number of k points used to sample the Brillouin zone varied from 1 to 32. Finally, the energy cut-off was raised to 15.2 Ryd. Based on this exploration, we conclude that the reconstruction energies are reasonably converged for supercells containing 96 atoms with sampling of four k points and at the energy cut-off of 11.1 Ryd. With these parameters, our value for the SP reconstruction energy still stands at 0.42 ± 0.04 eV per bond, about half that reported by Bigger *et al.* (1992). Presumably, the difference may be due to our use, in the present calculations, of an ultrasoft pseudopotential for silicon (Vanderbilt 1990) that is known to converge

at a much lower energy cut-off than the earlier pseudopotential schemes. We shall consider our value of 0.42 eV for the reconstruction energy to be sufficiently accurate for the subsequent discussion.

Having established numerical convergence for the case of SP reconstruction, we used the same computational settings to examine the DP reconstruction in the 90° partial. In agreement with Bennetto *et al.* (1997), the energy of the DP core structure came out lower than that of the SP reconstruction, by some 0.05 eV Å^{-1}. Recent calculations by Lehto and Oberg (1998) show that the magnitude and even sign of this relatively small energy difference between SP and DP cores depend on the supercell shape. Despite this subtle effect, our results appear accurate enough to conclude that, no matter which of the two reconstructions (SP or DP) is energetically favoured, the energy reduction caused by the core reconstruction of the 90° partial is significantly smaller than the corresponding value for the 30° partial. This offers a simple interpretation of the experimentally observed (Kolar *et al.* 1996) difference between mobilities of these two dislocations in silicon: the 30° partial is slower than the 90° partial since, in the former case, it takes more energy to break the stronger reconstruction bonds, as required for dislocation translation.

5.3. *Partial kink mechanisms*

Despite the lingering uncertainty just mentioned, all calculations reported so far show that SP and DP cores have very close, nearly degenerate energies (Bennetto *et al.* 1997, Valladares *et al.* 1998, Lehto and Oberg 1998). This implies that both SP and DP cores may be involved in dislocation translation. Because the spacing between two neighbouring SP and DP dislocation SGM positions is only half the regular spacing between the Peierls valleys in silicon 90° partials can presumably move in reduced 'steps'. First suggested by Bulatov *et al.* (1997) we now consider this possibility in some detail.

Let us assume, for our discussion, that the free energy of the DP core is lower than that of the SP core and that the difference is small. Consider now a kink by which a dislocation 'steps' from one DP valley to another (figure 10 (*a*)). The energy of this configuration can be reduced if the full kink dissociates into two kinks of half-height, separated by a short SP segment (figure 10 (*b*)). By analogy with partial dislocations in fcc, hcp and other materials, the half-kinks can be regarded as partial kinks and the short SP segment can be viewed as a one-dimensional stacking fault. The optimal dissociation width is determined by the competition of two energy terms. On the one hand, splitting of a full-height kink into two partial kinks reduces the elastic self-energy, which, for a kink of height h, is proportional to h^2. On the other hand, splitting introduces a one-dimensional stacking fault whose energy is proportional to its width. Neglecting for now the core terms, the energy of a dissociated pair of partial kinks can be estimated as

$$\Delta E(d) = \frac{\alpha \mu h^2 b^2}{d} + \gamma_1 d. \tag{1}$$

Here, the first term is the elastic repulsion between the partial kinks and contains the shear modulus μ, the height h of a full kink, the Burgers vector magnitude b and a numerical factor α that depends on the Poisson's ratio ν. The second term is the attractive 'glue' force in which $\gamma_1 = E_{sp} - E_{dp}$ is the one-dimensional stacking fault energy per unit length of the fault. The optimal splitting width is then given by

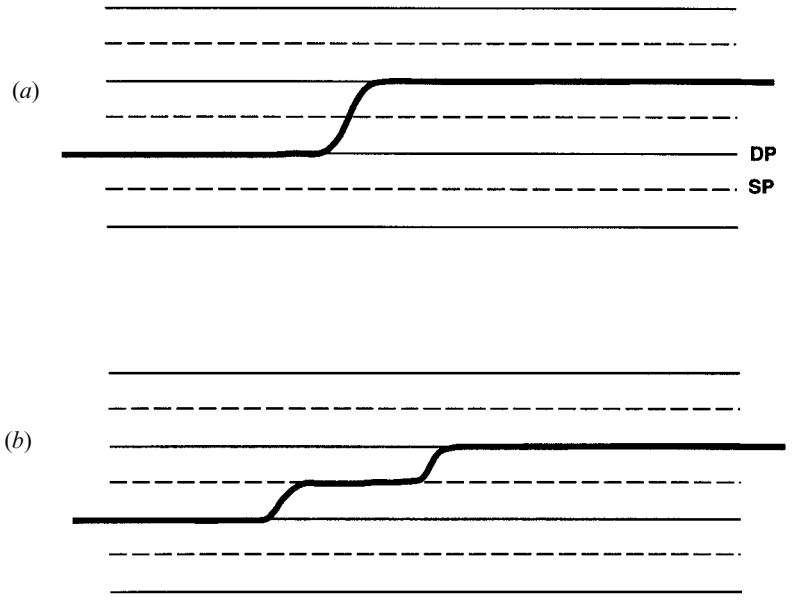

Figure 10. Dissociation of (*a*) a full kink into (*b*) two partial kinks connected by a one-dimensional stacking fault.

$$d_{min} = \left(\frac{\alpha \mu h^2 b^2}{\gamma_1} \right)^{1/2} . \tag{2}$$

Taking $\nu = 0.22$, $\alpha = 0.007\,14$, $\gamma_1 = 0.01\,\text{eV}\,\text{Å}^{-1}$, $\mu = 0.425\,\text{eV}\,\text{Å}^{-3}$, $b = 3.84\,\text{Å}$ and $h = 3.33\,\text{Å}$, the splitting width in the 90° partial in silicon can be estimated at 7 Å.

To verify that kink dissociation can indeed take place, we performed atomistic calculations, using the Tersoff (1986) interatomic potential that predicts $\gamma_1 = E_{sp} - E_{dp} = 0.01\,\text{eV}\,\text{Å}^{-1}$. To reduce the image effects we used large supercells containing up to 200 000 atoms. Fully relaxed atomistic configurations of the full and partial kinks are shown in figure 11. The energy difference between dissociated pairs of partial kinks and a full kink was calculated as a function of the width d of the partial kink pair. The results are shown in figure 12. The dissociated state has lower energy for kink separations ranging from 0 to 4b, with an optimum at around 2b. Thus, at least for the Tersoff model of silicon, kink dissociation is indeed favoured. According to equation (2), dissociation can be suppressed by a high value of γ_1 in which case d_{min} may become smaller than the core periodicity length (2b for the DP core). Although the dependence on γ_1 is rather weak (proportional to $\gamma_1^{-1/2}$), the remaining uncertainty in the value of γ_1 leaves it unclear whether partial kinks can contribute significantly to the motion of 90° partials. Lehto and Oberg (1998) have shown that the magnitude and even the sign of the energy difference between the SP and the DP core variants depend on stress exerted on the dislocation. This suggests an interesting possibility that, owing to the local stress variations, the energies of the two variants can become degenerate or nearly degenerate. In such conditions, kinks should dissociate.

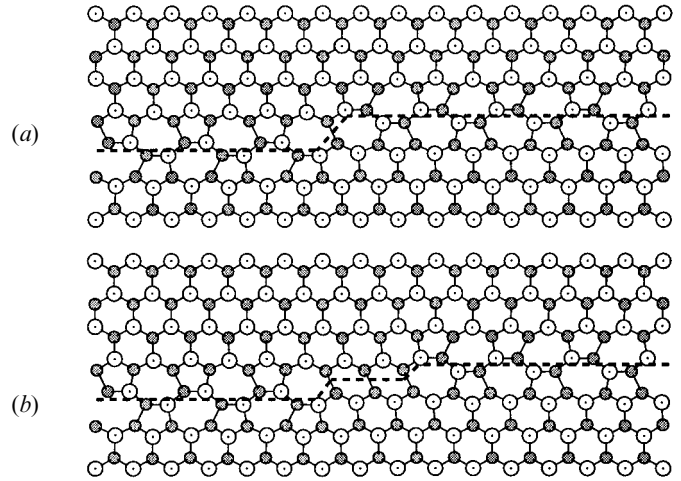

Figure 11. Actual atomic configurations of (*a*) a full kink and (*b*) partial kinks in a 90° partial dislocation.

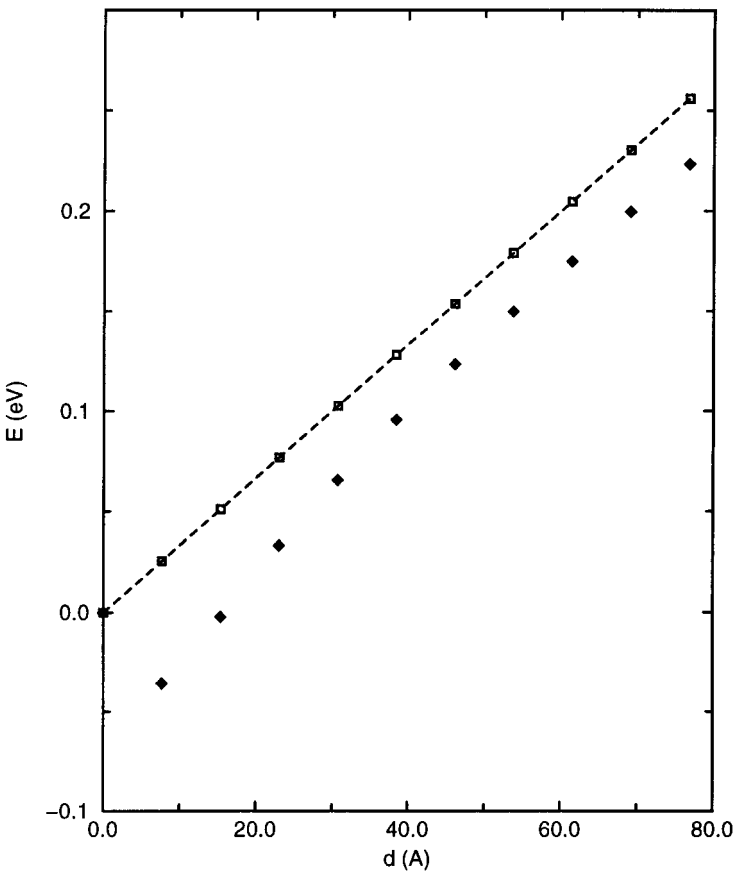

Figure 12. The energy of a dissociated pair of partial kinks over and above the energy of a full (undissociated) kink, as a function of splitting width d: (◆), energies calculated atomistically; (- - - -), as a reference, the 'glue' term $\gamma_1 d$.

The existence of partial kinks further enriches an already crowded spectrum of core defects involved in the motion of 90° partial dislocations in silicon. If the dissociation is indeed favoured, partial kinks can move sequentially, much like a pair of partial dislocations in fcc materials (we shall return to this in the following section) and, although our preliminary results are somewhat inconclusive, the partial kinks can be expected to have lower migration barriers than the full kinks. This is because translation of partial kinks involves smaller atomic displacements than a full kink case does. This way or another, the existence of two types of Peierls valley can be yet another reason, in addition to the weaker reconstruction bonds, why 90° partials have a higher mobility than 30° partials.

§ 6. Mesoscopic kinetic Monte Carlo simulations

Atomistic simulations provided much insight into the multiple and complex mechanisms of dislocation motion in silicon. At the same time, owing to the high barriers for kink nucleation and migration, MD simulations cannot be used for direct predictions of dislocation mobility. An alternative approach is to catalogue and characterize all the relevant atomic mechanisms involved in dislocation translation and to use these data to define a less detailed mesoscopic model that would be more computationally efficient. Our recent developments along these lines have been presented in the paper by Cai *et al.* (2000a).

In developing our mesoscopic model we tried to mimic the atomistic behaviour as closely as practically possible. Additionally, we included several realistic aspects of dislocation behaviour in silicon, such as dislocation dissociation and the existence of stacking faults, elastic interactions between kinks on both partials, and the thermally activated nature of kink nucleation and migration mechanisms. These realistic items were implemented in a kinetic Monte Carlo (kMC) procedure.

In principle, all the multiple atomic mechanisms of dislocation motion discussed in the preceding sections can be included in the catalogue of kMC events. However, for simplicity and in order to focus more on the effects of the interaction between two partials, we opted for a simplified description in which only one type of kink is considered. A more detailed approach in which multiple species of kinks can concurrently nucleate, migrate and react in response to stress and temperature will be reported elsewhere.

In our model, both partial dislocations are represented as piecewise straight continuous lines (figure 13). The horizontal (H) segments correspond to straight dislocations while the vertical (V) segments represent kinks. To account for the elastic interaction between partial dislocations and kinks, we implemented a full Peach–Koehler formalism to calculate stress exerted on each dislocation segment by all other dislocation segments. The rates of kink pair nucleation and kink migration events are calculated using the standard transition state theory equation (Cai *et al.* 1999) with the activation barriers imported from the atomistic calculations. Coupling to (local) stress is through a linear term equal to the work done by the local stress and the stacking-fault force on climbing up the activated (barrier) state.

The simulation proceeds as follows.

(1) For a given instantaneous configuration of the two partials, local stress on each segment (H and V) is computed as the sum of external and interaction stress.
(2) Rates for all kMC events allowed in the current configuration are computed.

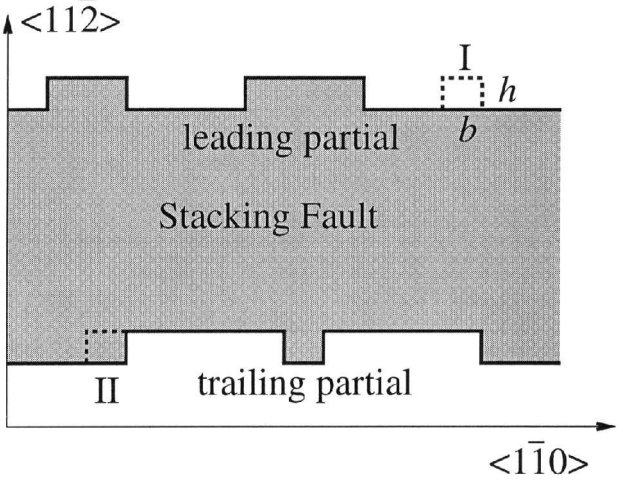

Figure 13. Schematic representation of a dislocation in silicon in the kMC simulation. The screw dislocation is dissociated into the leading and the trailing 30° partials, bounding an area of stacking fault. The elementary kink width is b and the kink height is h. A kink-pair formation event is shown at position I and a kink migration event is shown at position II, both as broken lines.

(3) A single event is randomly selected with probability proportional to its rate.
(4) Time is advanced by a small increment randomly selected according to the total 'evolution' rate.
(5) The selected event is executed and dislocation configuration is updated accordingly; return to step (1).

Under a constant external stress, the event probabilities become biased so that a directed motion of the dislocation pair is produced. The velocity is calculated as the slope of the instantaneous average displacement as a function of time. The model's predictions and their comparison with experimental data are shown in figures 14 and 15, for the screw dislocation in silicon. Two sets of simulated velocities shown in figure 14 were obtained using atomistic parameters obtained from two different models of silicon: the EDIP (Justo *et al.* 1998) and an O(N) TB approach (Bennetto *et al.* 1997). While neither of the two simulated curves agrees with the experiment too well, they appear to bracket the experiment, suggesting that the accuracy of the model is limited by the accuracy of its atomistic input.

The predicted stress dependence of dislocation velocity (figure 15) shows reasonable agreement with experiment with a linear dependence on stress above 25 MPa. At lower stresses, the so-called starting stress behaviour is also reproduced where the velocity increases sharply from very low values at low stresses (George 1979). This low-stress anomaly received considerable attention in the literature because linear velocity–stress dependence is expected from the simple kink diffusion model (Hirth and Lothe 1982). At the same time, some groups did report a perfectly linear stress dependence down to very low stress levels (Imai and Sumino 1983). Interestingly, our model reproduces both types of behaviour, depending on the material parameters.

Cai *et al.* (2000a) traced the lack or existence of a low stress anomaly to two distinctly different regimes of dislocation motion. In the first 'uncorrelated' regime, kink nucleation and migration events take place independently on two partials that

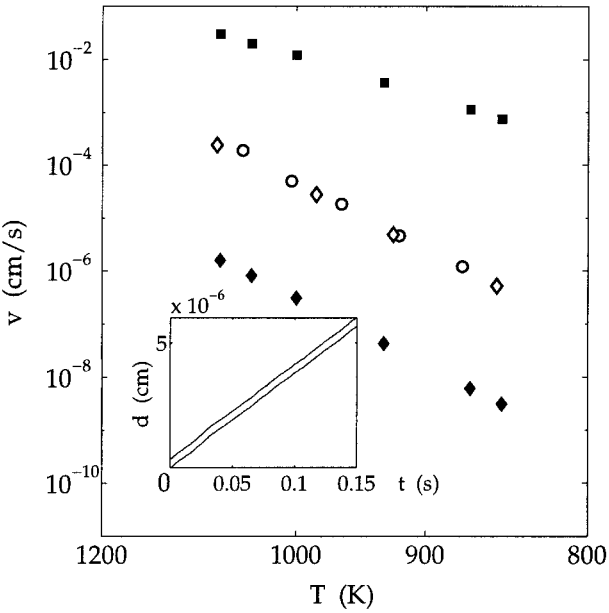

Figure 14. Temperature-dependent velocities of screw dislocations at stress $\tau = 10$ MPa: (◇) experiment data of George (1979); (○) experiment data of Imai and Sumino (1983); (■), kMC predictions using EDIP kink energetics; (◆), kMC predictions using TB kink energetics. The inset shows the simulated instantaneous positions of the two partials (see text).

move sequentially, one after another, producing nearly perfectly linear behaviour with no sign of low-stress anomaly. In the second 'correlated' regime, kink pairs have to form and propagate simultaneously on the neighbouring segments of two partials that now move in unison, producing a superlinear stress dependence at low stresses. At a stress above 25 MPa, correlations are totally suppressed and a linear regime sets in. Such a strongly correlated motion of two partials was first considered by Möller (1978). In our model, both uncorrelated and correlated regimes are reproduced depending on the value of the equilibrium dissociation width X_0. As explained by Cai *et al.* (2000a), the starting stress anomaly is observed when X_0 is integer in units of kink height h. On the other hand, when X_0 is a half-integer, no starting stress anomaly is observed. Since X_0 is a very sensitive function of the material parameters and local stress, even slight changes in the latter may change the low-stress behaviour dramatically. This may explain, at least partly, why several groups reported different low-stress behaviours and a large scatter of dislocation velocity data at low stresses. Furthermore, the demonstrated ability of our model to explain the low-stress anomaly raises questions about various *ad-hoc* entities such as 'weak obstacles' introduced earlier to explain the effect (Celli *et al.* 1963)†.

† A similar effect can be hypothesized for the case of dissociated kinks in the 90° partial discussed in the preceding section; the dissociated kinks may show an apparent starting stress behaviour when the ideal splitting distance d (equation (2)) is commensurate with the periodicity of the secondary Peierls potential opposing kink migration.

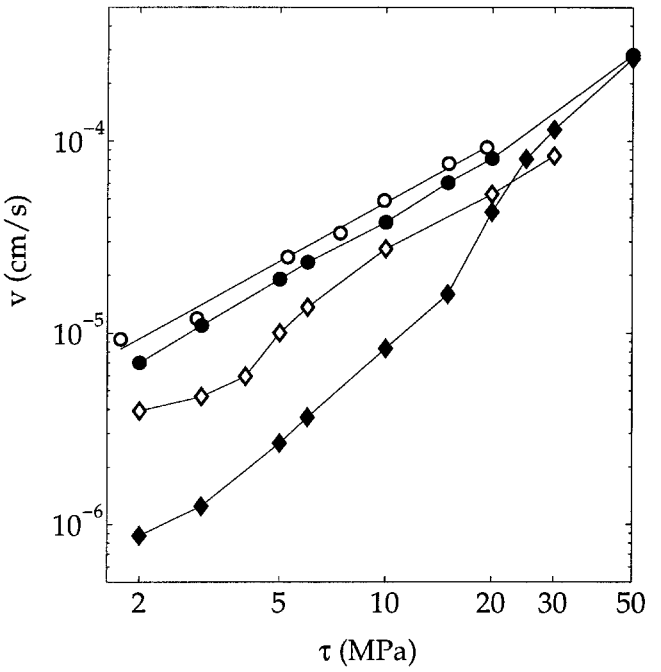

Figure 15. Velocity of a screw dislocation in silicon as a function of stress, at temperature $T = 1000$ K: (◆), kMC prediction for a commensurate case ($X_0 = 10.0h$), with a 'starting stress' at about 20 MPa; (◇), experimental data of George (1997) showing a similar velocity variation; (●), kMC results for a incommensurate case ($X_0 = 10.5h$), demonstrating a linear, stress–velocity relationship; (○), experimental data of Imai and Sumino (1983), which are in agreement with the kMC results for an incommensurate case.

The sensitivity to the parameter X_0 was used by Cai *et al.* (2000a) to examine dislocation mobility as a function of the (uniaxial) loading direction. For some orientations of the loading axis the non-glide (Escaig) components of external stress act to push the partials apart or to pull them together. Consequently, as the stress increases, the partials can pass through a sequence of 'integer' and 'half-integer' separations X_0 so that the resulting dependence on the total (glide + non-glide) stress can become oscillatory (figure 16). This prediction is now being investigated experimentally.

The ability of our mesoscopic model to incorporate the relevant atomistic details, combined with its computational efficiency, provides a bridge between the intricate physics of core mechanisms and dislocation mobility on the length and time scales readily accessible for experimental measurements. The accuracy of our combined atomistic–mesoscopic approach should be further tested against available experimental data. The model also predicts several unusual effects in dislocation mobility offered for experimental verification. In addition to the already mentioned 'integer–non-integer' transitions, we are exploring some unusual behaviours under oscillating and intermittent loading conditions and various asymmetries in the motion of mixed dislocations. These and other predictions will be presented elsewhere.

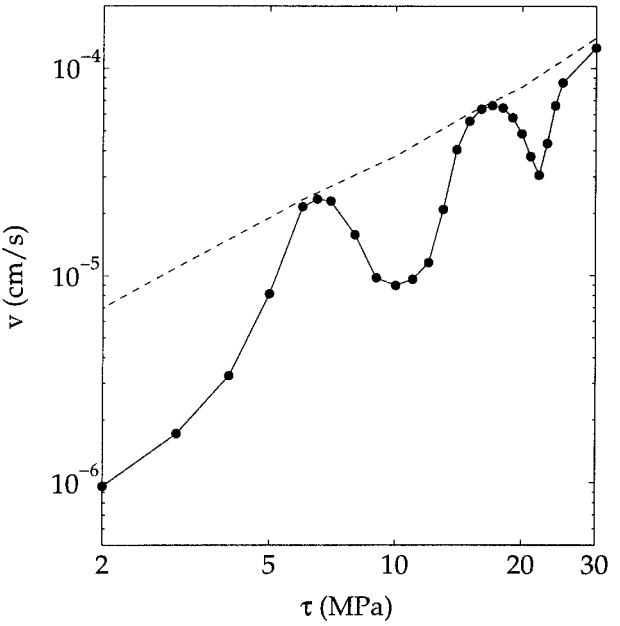

Figure 16. Dislocation velocity plotted against glide stress: (●), predicted for a special case when the ratio of the glide stress σ_{yz} to the non-glide stress σ_{xy} is fixed at -0.16; (- - - -), for comparison, dislocation velocity for an incommensurate case ($X_0 = 10.5h$) and zero non-glide stress.

§ 7. Summary

Our discussion has been focused on the issues that need to be addressed to obtain a parameter-free theoretical prediction of dislocation mobility in silicon. The approach presented here combines atomistic and mesoscopic (continuum) simulations covering a range of scales from ångstroms and picoseconds to tens of microns and seconds. The approach is parameter free in the sense that it does not involve any *ad-hoc* assumptions or parameter fitting. Equally important is the model's ability to predict new behaviour, to describe naturally some of the existing observations and to do away with some of the existing *ad-hoc* assumptions, for example 'weak obstacles'. At present, quantitative agreement between our simulations and the experiment is admittedly less impressive. This is an indication that, although our approach appears to capture the essential physics of dislocation motion silicon, its accuracy is still limited.

We see several reasons why our simulations may not agree with experiments. In addition to the previously mentioned inaccuracy of atomistic calculations, we have not taken into account several potentially important effects, such as the interaction between dislocations and intrinsic point defects and impurities and the effect of the Fermi level position on the charge state of the moving kinks (so far only the neutral states have been considered). However incomplete, our approach is operationally well defined and therefore can be systematically extended to incorporate these and other potentially important effects, if necessary. In view of the foregoing discussions, it seems clear that the path to further improvement will need to include more accurate atomistic data, kMC models with expanded catalogues of kink mechanisms, and direct comparisons with existing and future experiments.

Acknowledgements

We would like to thank A. P. Sutton and A. Valladares for kindly providing us with the coordinate files from the earlier DFT calculations (Bigger *et al*. 1992). This work has been supported over the years by an Office of Naval Research Coordinated Program on Mechanics and Atomistics of Mechanical Behavior, the National Science Foundation MRSEC Program at Massachusetts Institute of Technology, and the Lawrence Livermore National Laboratory under an ASCI-Level 2 award. Also, V.V.B., T.L. and T.D.R. acknowledge support from the Office of Basic Energy Sciences, the US Department of Energy and J.F.J. and M.K. acknowledge support from Fundação de Amparo a Pesquisa do Estado de São Paulo.

References

Alexander, H., and Teichler, H., 1993, *Mater. Sci. Technol.,* **4**, 249.
Bennetto, J., Nunes, R. W., and Vanderbilt, D., 1997, *Phys. Rev. Lett.,* **79**, 245.
Bigger, J. R. K., McInnes, D. A., Sutton, A. P., Page, M. C., Stich, I., King-Smith, R. D., Bird, D. M., and Clarke, L. J., 1992, *Phys. Rev. Lett.,* **69**, 2224.
Bourret, A., Thibault-Desseaux, J., and Lanaon, F., 1983, *J. Phys., Paris,* **44**, C4–15.
Bulatov, V. V., Justo, J. F., Cai, W., and Yip, S., 1997, *Phys. Rev. Lett.,* **79**, 5042.
Bulatov, V. V., Yip., S., and Argon, A. S., 1995, *Phil. Mag.* A, **72**, 453.
Cai, W., Bulatov, V. V., Justo, J. F., Argon, A. S., and Yip, S., 2000a, *Phys. Rev. Lett.,* **84**,3346.
Cai, W., Bulatov, V. V., and Yip, S., 1999, *J. Comput.-Aided Mater. Des.,* **6**, 175; 2000b (to be published).
Celli, V., Kabler, M., Ninomiya, T., and Thompson, R., 1963, *Phys. Rev.,* **131**, 58.
Csányi, G., Ismail-Beigi, S., and Arias. T. A., 1998, *Phys. Rev. Lett.,* **80**, 3984.
Deaven, D. M., and Ho, K. M., 1995, *Phys. Rev. Lett.,* **75**, 288.
Duesbery, M. S., 1983, *Acta metall.,* **31**, 1747.
Duesbery, M. S., and Joos, B., 1996, *Phil. Mag. Lett.,* **74**, 253.
Duesbery, M. S., Joos, B., and Michel, D. J., 1991, *Phys. Rev.* B, **43**, 5143.
Duesbery, M. S., and Richardson, G. Y., 1991, *CRC Crit. Rev. Solid St. Mater. Sci.,* **17**, 1.
George, A., 1979 *J. Phys. Paris,* **40**, 133.
Heggie, M., and Jones, R., 1983, *Phil. Mag.* B, **48**, 365; 1987, *Inst. Phys. Conf. Ser.,* **87**, § 5, 367.
Hirsch, P. B., 1979, *J. Phys., Paris,* **40**, C6–117.
Hirth, J. P., and Lothe, J., 1982, *Theory of Dislocations* (New York: Wiley), p. 373.
Imai, M., and Sumino, K., 1983, *Phil. Mag.* A, **47**, 599.
Justo, J. F., Bazant, M. Z., Kaxiras, E., Bulatov, V. V., and Yi, S., 1998, *Phys. Rev.* B, **58**, 2539.
Justo, J. F., Bulatov, V. V., and Yip, S., 1999, *J. appl. Phys.,* **86**, 4249.
Justo, J. F., de Koning, M., Cai, W., and Bulatov, V. V., 2000, *Phys. Rev. Lett.,* **84**, 2172.
Kaxiras, E., and Duesbery, M. S., 1993, *Phys. Rev Lett.,* **70**, 3752.
Keating, P. N., 1966, *Phys. Rev.,* **145**, 647.
Kirchner, H. O. K., and Suzuki, T., 1998, *Acta mater.,* **46**, 305.
Kirkpatrick, S., 1984, *J. statist. Phys.,* **34**, 975.
Kolar, H. R., Spence, J. C. H., and Alexander, H., 1996, *Phys. Rev. Lett.,* **77**, 4031.
Kresse, G., and Hafner, J., 1993, *Phys. Rev.* B, **47**, RC558; 1994, *J. Phys.: condens. Matter,* **6**, 8425.
Lehto, N., and Heggie, M. I., 1998, *Properties of Crystalline Silicon,* edited by R. Hull, EMIS Datareviews Series, Vol. 20 (London: INSPEC). p. 357.
Lehto, N., and Ober, S., 1998, *Phys. Rev. Lett.,* **80**, 5568.
Louchet, F., and Thibault-Desseaux, J., 1987, *Rev. Phys. Appl.,* **22**, 207.
Möller, H. J., 1978, *Acta metall.,* **26**, 963.
Nunes, R. W., Bennetto, J., and Vanderbilt, D., 1996, *Phys. Rev. Lett.,* **77**, 1516; 1998, *Phys. Rev.* B, **57**, 10 388.
Olsen, A., and Spence, J. C. H., 1981, *Phil. Mag.* A, **43**, 945.
Parrinello, M., and Rahman, A., 1982, *J. chem. Phys.,* **76**, 2662.

POND, R. C., 1989, *Dislocations in Solids,* Vol. 8, edited by F. R. N. Nabarro (Amsterdam: North-Holland), p. 1.
STILLINGER, F. H., and WEBER, T. A., 1985, *Phys. Rev.* B, **31**, 5262.
TERSOFF, J., 1986, *Phys. Rev. Lett.,* **56**, 632.
VALLADARES, A., WHITE, J. A., and SUTTON, A., 1998, *Phys. Rev. Lett.,* **81**, 4903.
VANDERBILT, D., 1990, *Phys. Rev.* B, **41**, 7892.
WOOTEN, F., WINER, K., and WEAIRE, D., 1985, *Phys. Rev. Lett.,* **54**, 1392.